Chalcogenide Letters Vol. 21, No. 5, May 2024, p. 395- 405

Tribological properties of ternary heterojunction nanocomposites with MoS_2 as the main body are enhanced

X. Y. Gao*, P. Lu, Z. M. Xu, G. G. Tang
Changzhou Vocational Institute of Industry Technology, Changzhou, 213100, Jiangsu Province, China

$g\text{-}C_3N_4$ has a strong C-N covalent bond within the monolayer and a weak van der Waals force between the lamels, which enables it to have similar lubrication properties to other two-dimensional layered materials. In this study, a new type of $g\text{-}C_3N_4/MoS_2/ZnS$ heterogeneous nanocomposites was prepared by a one-step hydrothermal method XRD, SEM, FI-IR, and other methods were used to systematically study it. Furthermore, a ball-on-disk tribometer extensively examined the tribological behavior of $g\text{-}C_3N_4/MoS_2/ZnS$ heterojunction in pure oil. The relationship between applied load and rotational speed on performance is also revealed. Compared with $g\text{-}C_3N_4$ and $g\text{-}C_3N_4/MoS_2$ nanocomposites, $g\text{-}C_3N_4/MoS_2/ZnS$ has better frictional properties. It is worth noting that when $g\text{-}C_3N_4/MoS_2/ZnS$ is in the base oil mass ratio at 1.0 wt.%, the friction coefficient is reduced by 49%. In addition, $g\text{-}C_3N_4/MoS_2/ZnS$ ternary heterojunction exhibits better tribological properties than $g\text{-}C_3N_4/MoS_2/ZnS$ mixture, expanding their practical applications in industry and agriculture.

(Received February 2, 2024; Accepted May 9, 2024)

Keywords: MoS_2, Heterojunction, 2D/2D structure, Tribological properties

1. Introduction

$g\text{-}C_3N_4$ nanosheets, like graphene, have a large surface area and are often used as carrier materials, and there are a large number of hydrogen elements in the form of primary and/or secondary amine groups at the end edge of $g\text{-}C_3N_4$ lamellar structure, which leads to a good deal of defect active sites on the surface of the lamellar structure[1-3]. These defect-active sites are very favorable for the recombination of $g\text{-}C_3N_4$ with other nanoparticles[4]. In recent years, a large number of researchers have reported relevant studies on $g\text{-}C_3N_4$-based nanocomposites, such as $g\text{-}C_3N_4/Au$[5], $g\text{-}C_3N_4/MoO_3$[6], $g\text{-}C_3N_4/TiO_2$[7], $g\text{-}C_3N_4/MoS_2$[8], $g\text{-}C_3N_4/WS_2$[9], $g\text{-}C_3N_4/MoS_2/TiO_2$[10], etc. Although these nanocomposites have ideal heterogeneous structures, the research on their application is almost only involved in the field of catalysis, and the application in the field of tribology is almost blank. At the same time, compared with graphene materials, $g\text{-}C_3N_4$ has more advantages in terms of price, synthesis process, and yield. Therefore, the research of $g\text{-}C_3N_4$-based nanocomposites as lubricating oil additives will gradually emerge.

* Corresponding author: gaoxy_2023@163.com
https://doi.org/10.15251/CL.2024.215.395

In the TMDCs family, transition metal sulfide MS_2 has received continuous research and attention from researchers in various fields [11-14]. Among them, MoS_2 is a very typical representative of transition metal sulfide, which belongs to the hexagonal crystal system layer structure. MoS_2 crystal is composed of an "S-Mo-S" unit layer, between layer and layer is a weak van der Waals molecular force connected, which makes MoS_2 layer and layer easily stripped, so MoS_2 has excellent lubrication performance and is one of the most widely used lubricant materials at present [15-20]. Many studies have also shown that nanoscale MoS_2 has more outstanding tribological properties than ordinary MoS_2, and as an additive added to lubricating oil can greatly improve the performance of lubricating oil, which is worthy of our further exploration. ZnS is usually used as a lubricant additive to achieve its lubrication effect, and it has two kinds of structure, sphalerite type (cubic, β phase) and wurtzite type (hexagonal structure, α phase), and excellent friction properties [21], and is widely used in many fields, especially in the field of tribology[22-23]. For example, Rukiye et al[24] research presented the frictional properties of ZnS nanoparticles, and the results showed that ZnS nanomaterials have good lubrication ability in the process of stick-slip movement at the friction interface. At the same time, Liu[25] studies the tribological properties of ZnS nanoparticles added to lubricating oil, and the test results show that ZnS nanoparticles can significantly improve the friction and wear properties of lubricating oil. Herein, a novel g-C_3N_4/MoS_2/ZnS ternary heterojunction was prepared by a one-step solvothermal method. The tribological and wear properties were compared using a ball-and-disc tribometer. Additionally, the wear trajectory was characterized in terms of its morphology and composition using SEM, SMP, and EDX techniques to gain insights into the friction and wear mechanism. Consequently, the structure and exceptional tribological properties of g-C_3N_4/MoS_2/ZnS heterojunction will facilitate the design of novel nano additives with ternary heterojunction structure to enhance anti-friction and anti-wear properties while expanding its application in industry or agriculture.

2. Experimental

2.1. Synthesis of g-C_3N_4/MoS_2/ZnS

The synthesis of g-C_3N_4/MoS_2/ZnS ternary nanocomposites also adopts a simple and effective hydrothermal synthesis method. Specific steps are as follows: First, g-C_3N_4 nanosheets are prepared by the method described in 3.2.2.1. Then, the prepared g-C_3N_4 was added to 50 ml deionized water by weighing 0.20 g and ultrasonic treatment for 1 h to prepare the g-C_3N_4 dispersion solution. Then, according to $Na_2MoO_4{\cdot}2H_2O$: $ZnSO_4{\cdot}7H_2O$: $HONH_3Cl$= 1:1: For the molar ratio of 2.2, 0.4698 g $Na_2MoO_4{\cdot}2H_2O$, 0.5583 g $ZnSO_4{\cdot}7H_2O$, 0.2968 g $HONH_3Cl$ were added to g-C_3N_4 dispersion solution and stirred magnetically for 10 min. Finally, according to the molar ratio of Mo: S= 1:3, 0.4376 g C_2H_5NS was weighed and dissolved in 10 mL deionized water to obtain thioacetamide solution, which was added to the above-mentioned dispersion by drops at the rate of 1 drop/s with a dropper, and pH= 6 was adjusted with 2 mol/L hydrochloric acid solution. Stir continuously for 0.5 h, transfer the above-mixed solution to the hydrothermal reactor, seal it, place the reactor in the oven, and react at 180 ℃ for 24 h. The obtained products were washed three times and washed three times with alcohol. Finally, vacuum drying at 60 ℃ for 12 h, to obtain g-C_3N_4/MoS_2/ZnS nanocomposites denoted as CNMZ.

2.2. Characterization

The phase composition, chemical state, and microstructure of the products were analyzed by XRD (X-ray diffractometer) with a Bruker-AXS instrument, Raman microscopy with a DXR-Thermo Scientific instrument, SEM (scanning electron microscopy) with a JEOL JXA-840A instrument, and TEM (transmission electron microscopy) with a JEOL JEM-2100 instrument.

2.3. Tribological test

The antifriction and anti-wear performance of different additives in the pure base oil is based on the ball-and-disc tribometer (MS-T3001, China). In our experimental setup, pure oil was employed as the lubricating agent. The steel ball's rotational speed was maintained at 300 RPM, while an applied load of 6 N was exerted for 0.5 hours at room temperature. Furthermore, we studied the addition of CNMS (0.5-2.5 wt.%) without concentration, rotational speed (100-400 rpm), and applied force (4-10 N). Additionally, all friction experiments were conducted thrice independently.

3. Results and discussion

To confirm the synthesis of g-C_3N_4/MoS_2/ZnS composites, the prepared samples were analyzed by XRD. The XRD pattern from g-C_3N_4 is consistent with the previous results (Fig. 1)[26]. According to the XRD pattern of the prepared MoS_2, the main diffraction peaks correspond well corresponding to the standard characteristic peaks of the hexagonal MoS_2 crystal (JCPDS No. 37-1492). It can be seen from the XRD pattern of ZnS that the hydrothermal preparation of ZnS has a high crystallinity, all the diffraction peaks are well corresponding to the standard pattern of ZnS crystals with cubic structure (JCPDS No. 65-0309), and no other stray peaks. In addition, The XRD pattern of g-C_3N_4/MoS_2/ZnS composite simultaneously shows the main characteristic diffraction peaks of g-C_3N_4, MoS_2, and ZnS, which can be preliminarily inferred that the successful preparation of this terpolymer. It is worth noting that after the introduction of g-C_3N_4 nanosheets, the intensity of all diffraction peaks in the XRD pattern of CNMZ is slightly lower than that of its single phase, which indicates that the steric hindrance effect between the three substances during the formation of the composite effectively hinders the aggregation and self-assembly of its single phase. At the same time, the introduction of g-C_3N_4 significantly inhibits the rapid growth of MoS_2 and ZnS crystals in the composite, thus obtaining smaller nanostructures. In addition, the diffraction peak of g-C_3N_4 in the composite is weak, which is mainly due to the low content of g-C_3N_4 and its small diffraction peak intensity.

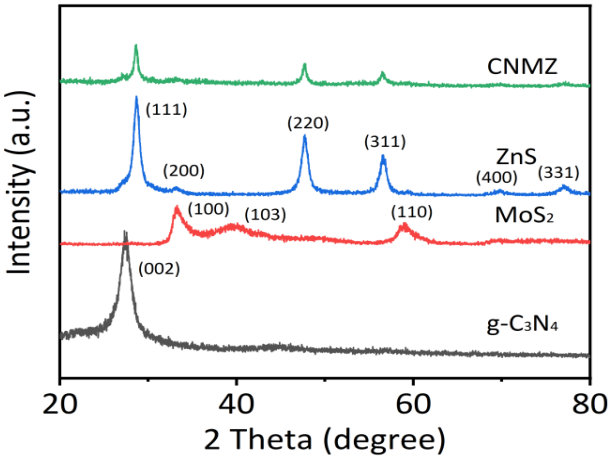

Fig. 1. XRD test results of g-C_3N_4, MoS_2, ZnS, and CNMZ.

Fig. 2 shows the infrared spectra of g-C_3N_4, MoS_2, ZnS, and CNMZ nanocomposites. For pure MoS_2 and pure ZnS, the infrared spectra of both are very similar. The difference is that the infrared spectrum of MoS_2 has a weak characteristic absorption peak at about 595 cm^{-1}, and the vibration is consistent with the Mo-S bond [27-29]. However, due to the high infrared transmittance of ZnS nanoparticles[30-31], no characteristic absorption peak was detected in the infrared spectra of pure ZnS, and other absorption peaks of the two spectra may be attributed to the influence of exogenous groups or residual groups of reaction raw materials[29]. For pure g-C_3N_4, the characteristic peak in the range of 1243-1636 cm^{-1}, belongs to the stretching vibration of carbon-nitrogen aromatic heterocyclic compounds, and the peak at 809 cm^{-1} is attributed to the respiratory vibration mode or the out-of-plane bending vibration mode of the isotriazine unit[32]. Stretching vibrations corresponding to N-H and O-H bonds in the range of 3100-3500 cm^{-1} are mainly due to uncondensed amino groups and surface adsorption of water[33].

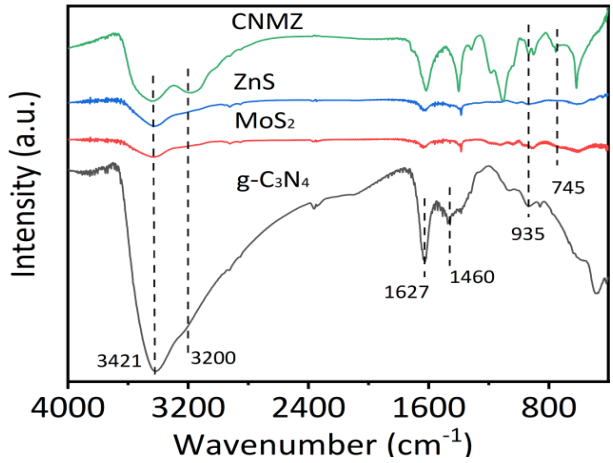

Fig. 2. FT-IR test results of MoS_2, ZnS, g-C_3N_4, and CNMZ.

In particular, the infrared spectrum of CNMZ composite has a large gap with that of pure g-C_3N_4, indicating that the heterogeneous hybridization among MoS_2, g-C_3N_4, and ZnS significantly weakens the vibration of aromatic heterocyclic compounds after the introduction of MoS_2 and ZnS. However, it is worth noting that the infrared spectrum of CNMZ composite still has the typical characteristic absorption peak of g-C_3N_4 at 809 cm^{-1}, while the weak characteristic peak of MoS_2 is also detected at 595 cm^{-1}. Combined with XRD analysis, it can be inferred that g-C_3N_4/MoS_2/ZnS heterojunctions have been successfully prepared.

Fig. 3 shows the SEM and TEM images of MoS_2, ZnS, and CNMZ nanocomposites and the synthesis mechanism of CNMZ. As shown in Fig. 3a, pure MoS_2 appears spheroidal, self-assembled from its nanosheets, with an average size of about 1 μm and significant agglomeration. Fig. 3b shows the SEM images of pure ZnS. It can be seen that ZnS appear as large and non-uniform hollow microspheres, which are self-assembled by smaller ZnS nanoparticles. Fig. 3c is the SEM image of CNMZ nanocomposites, from which it can be seen that g-C_3N_4, MoS_2, and ZnS form an ideal heterostructure, and neither ZnS nor MoS_2 has a self-assembled three-dimensional structure, and smaller ZnS nanoparticles are attached to g-C_3N_4 or MoS_2 nanosheets. The heterogeneous structures were uniformly dispersed and agglomeration did not occur. Fig. 3d is the TEM image of CNMZ nanocomposites. It can be seen that most ZnS nanoparticles and MoS_2 nanosheets are attached to g-C_3N_4 nanosheets, and g-C_3N_4 nanosheets hinder the self-assembly and agglomeration of MoS_2 and ZnS, indicating that it has a small thickness size. Indicating that g-C_3N_4/MoS_2/ZnS nanocomposites have been successfully synthesized by this hydrothermal method.

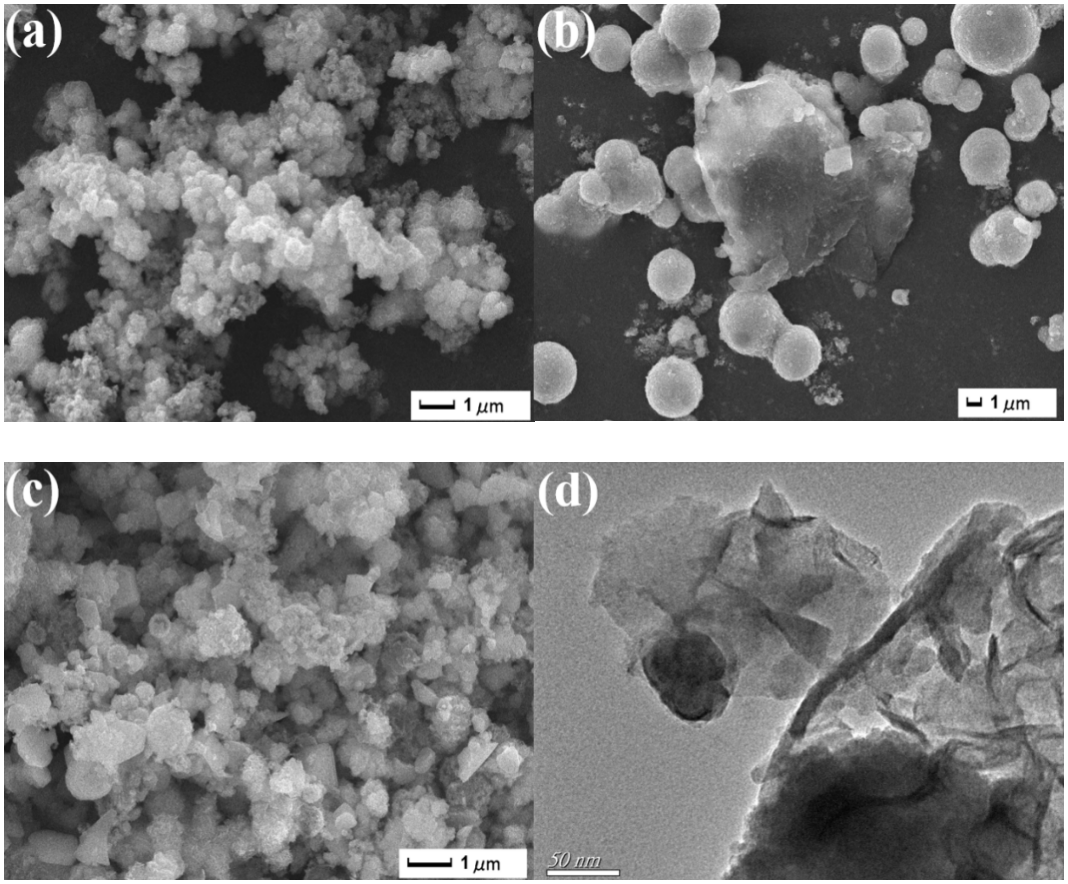

Fig. 3. Scanning electron microscope (SEM) test results of (a) MoS_2, (b) ZnS, (c) CNMZ nanocomposites; (d) Transmission electron microscope (TEM) images of CNMZ nanocomposites.

Different sulfur sources have important effects on the morphology of transition metal sulfides synthesized by hydrothermal synthesis. For the hydrothermal synthesis system of CNMZ, the products synthesized with different sulfur sources have different structural characteristics. The sulfur source used in the previous study was C_2H_5NS, and the ideal CNMZ heterostructure was obtained. Therefore, under the same experimental conditions, we chose thiourea and sodium sulfide as sulfur sources for comparative analysis. Fig. 4a-b is the SEM image of CNMZ prepared by using CH_4N_2S as a sulfur source. It can be seen from the figure that both MoS_2 and ZnS are self-assembled, and ZnS is a large microsphere with a diameter of about 6-7 μm, while MoS_2 has a variety of structural characteristics, most of which are flower spherical structures. At the same time, some irregular aggregates formed by g-C_3N_4 and MoS_2 were also observed, and some MoS_2 assembly structures tended to be coated with ZnS microspheres. Fig. 4c-d is the SEM image of CNMZ prepared by using $Na_2S·9H_2O$ as a sulfur source, from which a large number of large-size self-assembled microspheres can be seen. In the SEM image of high power, it is found that there is a large number of debris on the surface of the microspheres, and these microspheres are mainly assembled by ZnS, making it difficult to identify the presence of MoS_2. The reason may be that the strong chemical activity of $Na_2S·9H_2O$ causes the rapid nucleation, growth, and self-assembly of ZnS, and seriously deprives MoS_2 of the necessary sulfur source. In summary, it can be concluded that both thiourea and sodium sulfide are not conducive to the formation of ideal CNMZ heterojunctions, and their structural characteristics are not conducive to improving the lubrication performance of lubricating oil. Therefore, it is crucial to select a suitable sulfur source for the formation of ideal CNMZ.

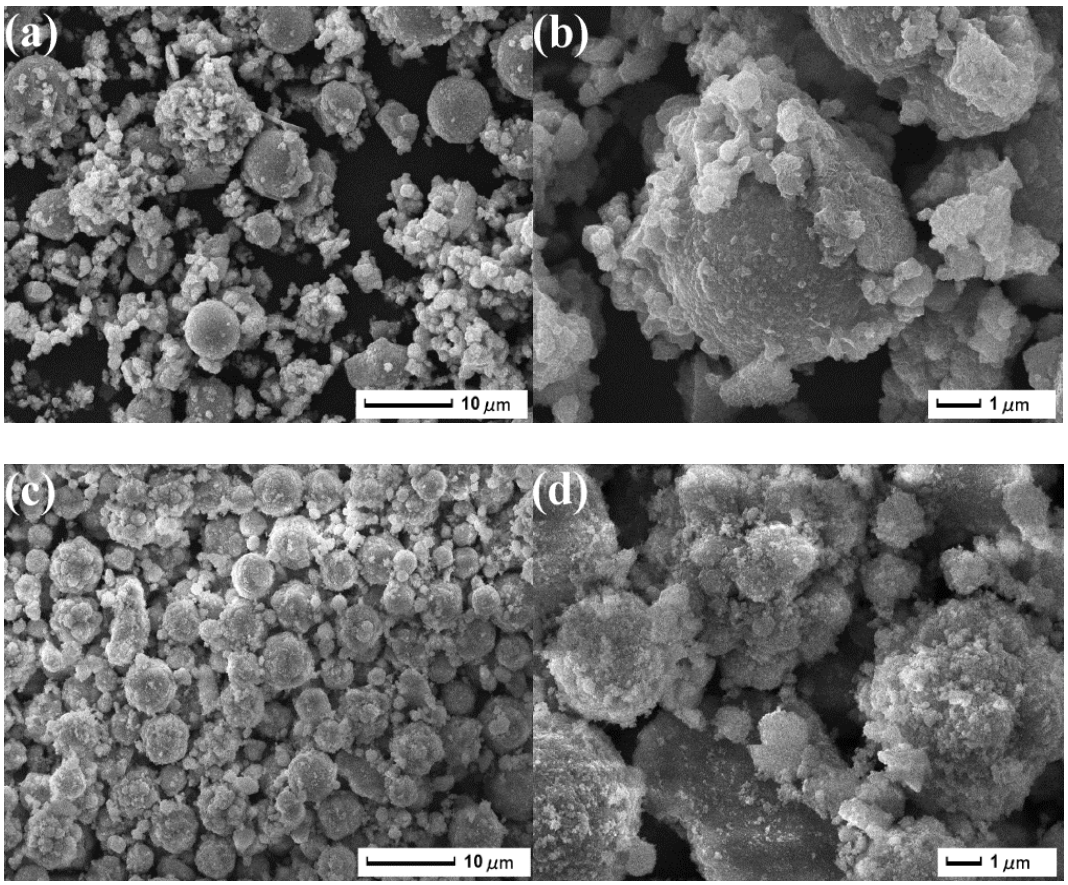

Fig. 4. SEM images of CNMZ obtained at various sulfur sources: (a, b) thiourea (CH_4N_2S), (c, d) sodium sulfide nonahydrate ($Na_2S·9H_2O$).

To study the tribological properties of CNMZ nanocomposites, CNMZ nanocomposites (1.0 wt.%) and dispersant span-80 (1.0% volume ratio) were mixed into liquid paraffin base oil and dispersed by ultrasonic for 30 min to obtain a uniform and stable dispersion system. To verify the tribological properties of the composite, the friction coefficient of the CNMZ mixed oil sample and the wear rate of the steel disc were tested. As a comparison, the lubrication behavior of pure paraffin oil, paraffin oil containing g-C_3N_4, and paraffin oil containing g-C_3N_4+MoS_2+ZnS mixture was tested at the same time (load 20 N, reciprocating speed 200 rpm, and so on). Time: 10 min/ time). Fig. 5a shows the typical friction coefficient curve of pure paraffin oil and CNMZ mixed oil sample sample sample samples. According to the diagram during the test period, the lubrication process of CNMZ mixed oil samples entered a stable lubrication and friction reduction stage after a short period of adjustment, while the friction coefficient of pure paraffin oil during the lubrication process was larger and theirthere was greater instability. As can be seen from the bar chart in Fig. 5a, andthe average friction coefficient of lubricants containing additives (g-C_3N_4, g-C_3N_4+MoS_2+ZnS mixture, CNMZ) is significantly lower than that of pure paraffin oil, and the wear rate shows similar results (Fig. 5b). However, it is worth noting that the CNMZ mixed oil sample has the lowest average friction coefficient (reduced by about 49%) and wear rate (reduced by about 68%), and combined with its stable friction coefficient curve, it can be concluded that the CNMZ nanocomposite exhibits the best lubrication performance. The excellent antifriction and anti-wear properties of CNMZ in base oil may be attributed to its ideal ternary heterostructure and the effective synergistic effect among g-C_3N_4 flakes, MoS_2 nanosheets, and ZnS nanoparticles. The lubrication mechanism of the mixture of CNMZ and g-C_3N_4+MoS_2+ZnS is different. Combined with the microstructure analysis in Fig. 4, the self-assembly structure of pure MoS_2 and ZnS prepared by the same method is larger, which greatly limits their tribological properties, and the simple mixing of the three substances cannot show effective synergies.

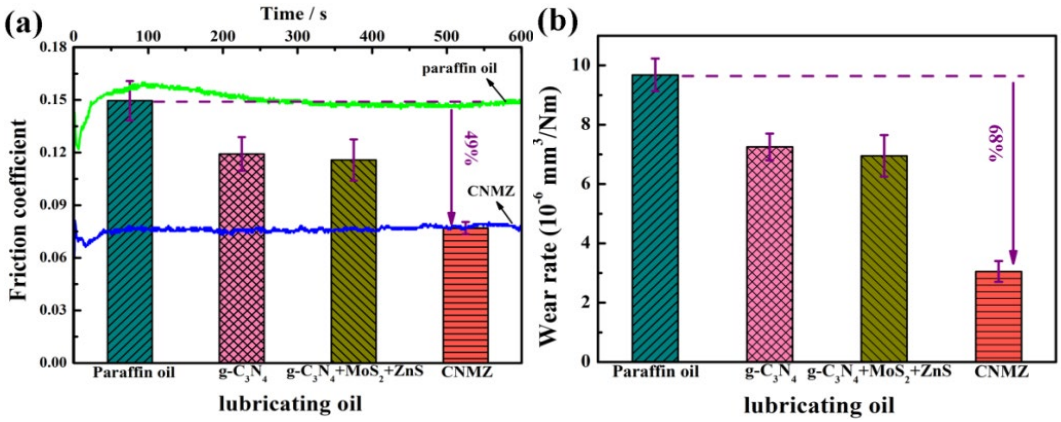

Fig. 5. (a) The average friction coefficient and (b) the average wear rate of pure paraffin oil and base oil with different additives were measured (g-C_3N_4、g-C_3N_4+MoS_2+ZnS mixture and CNMZ nanocomposite). The insert line in (a) shows the change in the coefficient of friction over time between paraffin oil and paraffin oil containing 1.0 wt.% CNMZ at 20 N. (Load: 20 N, Rotational speed: 200 rpm, Time: 10 min).

Fig. 6a and b show the average friction and average wear rate of different lubricating oil samples under different loads (load: 5-30 N, reciprocating speed: 200 rpm, time: 10 min/ time). As can be seen from Fig. 6a, lubricants containing additives show a lower mean coefficient of friction than pure paraffin oil at all test loads, and the corresponding wear rate of 45# steel shows the same result (Fig. 6b). In addition, under the test load, the lubrication effect of CNMZ in the base oil is better than that of g-C_3N_4 and g-C_3N_4+MoS_2+ZnS mixtures alone, the average friction coefficient is reduced by at least 40%, the average wear rate is reduced by at least 65%, and the reduction degree is the largest. This indicates that CNMZ can enhance the antifriction and antiwear properties of base oil more effectively. According to SEM and TEM results, we know that in CNMZ composites, MoS_2 has a very thin sheet structure, and ZnS particles have a smaller particle size. MoS_2 nanosheets and spherical ZnS particles attached to g-C_3N_4 flakes can more easily enter the contact space of friction parts and constantly repair the worn interface (MoS_2 nanosheets are more likely to form a lubricating transfer film, and ZnS nanoparticles play the role of nano bearings). After the run-in period, it is easier to form a continuous composite lubricating protective film on the contact surface, so that CNMZ shows better anti-friction and anti-wear performance.

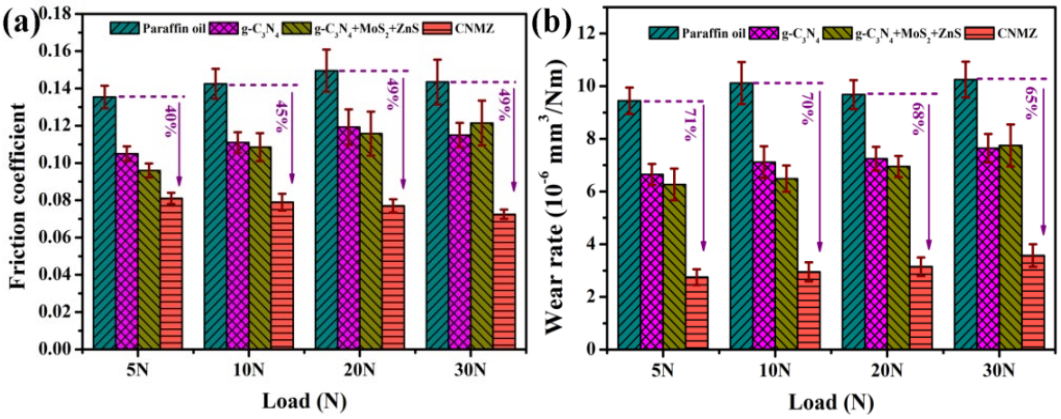

Fig. 6. (a) Average friction coefficient and (b) average wear volumes at 5, 10, 20, and 30 N of steel/steel contacts lubricated with paraffin oil and oil with g-C_3N_4, g-C_3N_4+MoS_2+ZnS mixture, oil with CNMZ nanocomposite at room temperature.

To further evaluate the wear resistance of CNMZ as a lubricant additive, the surface morphology of the wear marks was analyzed by SEM and non-contact ultra-depth field three-dimensional microscopy. Fig. 7 shows the SEM diagram, 3D profile diagram, and cross-sectional section file of the wear marks formed by the lubricating oil containing different additives (1.0 wt.% g-C_3N_4+MoS_2+ZnS mixture, 1.0 wt.% CNMZ nanocomposite) after friction test (experimental conditions: Load: 20 N, speed: 200 rpm, time: 10 min). From the analysis of Fig. 7a-c, we have concluded that pure paraffin oil has poor anti-wear properties. When the mixture of g-C_3N_4+MoS_2+ZnS (Fig. 7a-c) is added to paraffin oil, there are many small pits and irregular scratching on the surface of the wear marks, accompanied by relatively serious plastic deformation, adhesion, and abrasive wear. The research results show that the mixture of g-C_3N_4+MoS_2+ZnS has limited lubrication and anti-wear effect. And simple material mixing can not achieve the ideal effect of enhancing lubrication. More importantly, when the CNMZ nanocomposites were added to the paraffin oil (Fig. 7d-f), not only did the width and depth of the wear marks become significantly smaller, but the surface of the wear marks also became quite smooth, with only fine grooving and slight plastic deformation, indicating that the CNMZ nanocomposites had the best anti-wear properties. The above results are consistent with the friction test results in Fig. 5 and Fig.

6 above The friction coefficient of lubricating oil with 1.0 wt.% g-C_3N_4+MoS_2+ZnS mixture decreased by 37%, and that with 1.0 wt.% CNMZ decreased by 49%. Combined with Fig. 7d-f, the friction coefficient of lubricating oil with 1.0 wt.% CNMZ decreased by 49%. The results confirmed that there was no significant difference between the two wear marks, but the wear marks after CNMZ lubrication were significantly narrower and shallower. It can be preliminarily inferred that the ternary heterojunction of CNMZ exhibits better tribological properties and further research is needed.

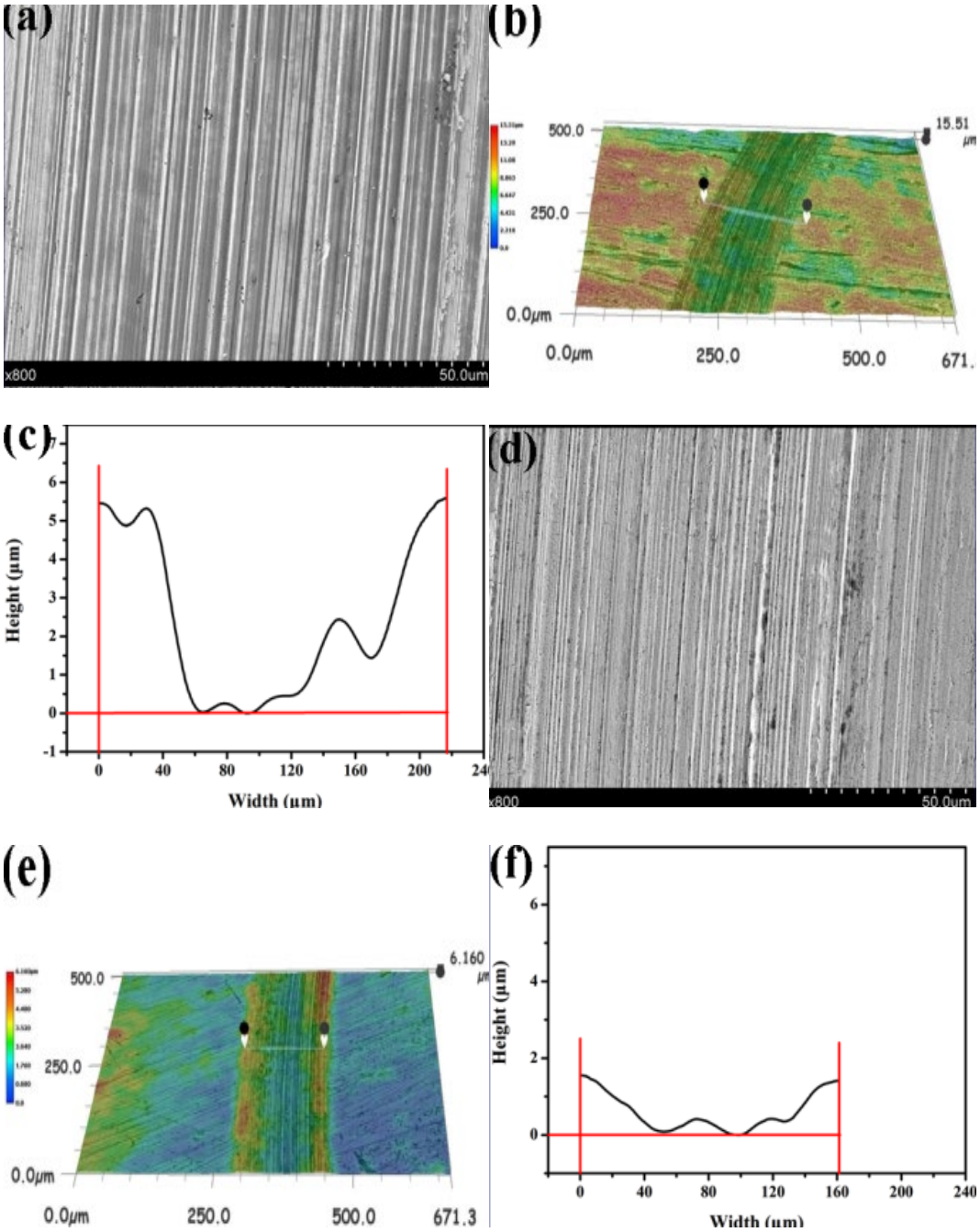

Fig. 7. The g-C_3N_4+MoS_2+ZnS mixture oil (a, b) was utilized for the analysis of the wear surface of lubricated steel through SEM imaging (a, d), and to generate a non-contact 3D image of the wear trajectory (b, e), and (d, e) oil with CNMZ nanocomposite. The cross-sectional profile corresponding to the wear trajectory at points (c, f) can be visually represented as a three-dimensional image.

4. Conclusions

The g-C_3N_4/MoS_2/ZnS nanocomposites were obtained by a simple hydrothermal method. The results show that adding graphite phase carbon nitride can effectively prevent the formation of large-scale self-assembled structures of MoS_2 and ZnS, and the steric hindrance effect causes g-C_3N_4, MoS_2, and ZnS to form a relatively ideal heterogeneous structure. MoS_2 and ZnS are attached to g-C_3N_4 nanosheets in the form of nanosheets and nanoparticles, respectively. At the same time, the influence of sulfur source on the morphology of CNMZ was investigated, and it was concluded that thiourea and sodium sulfide were not conducive to the formation of ideal CNMZ heterojunction. The tribological properties of CNMZ nanocomposites were investigated as an additive in lubricating oil using the UMT-2. Reveal compared with paraffin oil and mixed oil samples containing g-C_3N_4, g-C_3N_4+MoS_2+ZnS, CNMZ blends exhibit the lowest average friction and wear rate. It has better anti-friction and anti-wear properties. In the friction process, the effective synergistic effect of g-C_3N_4, MoS_2, and ZnS in the CNMZ nanocomposite has improved the lubrication effect, while the simple materials do not yield significant improvements in lubrication. In addition, CNMZ ternary nanostructures exhibit better tribological properties than g-C_3N_4/MoS_2/ZnS mixture.

References

[1] Y.L. Ma, Y.Y. Tao, Chalcogenide Lett. 20 (2023) 153-164; https://doi.org/10.15251/CL.2023.202.153

[2] W.J. Ong, L.L. Tan, Y.H. Ng, S.T. Yong, S.P. Chai, Chem. Rev. 116 (2016) 7159; https://doi.org/10.1021/acs.chemrev.6b00075

[3] L. Zhu, Y. Wang, F. Hu, H. Song, Appl. Surf. Sci. 345 (2015) 349-354; https://doi.org/10.1016/j.apsusc.2015.03.197

[4] Z. Zhao, Y. Sun, F. Dong, Nanoscale. 7 (2015) 15-37; https://doi.org/10.1039/C4NR03008G

[5] H. Zhu, X. Chen, Z. Zheng, X. Ke, E. Jaatinen, J. Zhao, D. Wang, Chem. Commun. 48 (2009): 7524-7526; https://doi.org/10.1039/b917052a

[6] L. Huang, H. Xu, R. Zhang, X. Cheng, J. Xia, Y. Xu, H. Li, Appl. Surf. Sci. 283 (2013) 25-32; https://doi.org/10.1016/j.apsusc.2013.05.106

[7] K. Sridharan, E. Jang, T. J. Park, Appl. Catal. B. 142 (2013) 718-728; https://doi.org/10.1016/j.apcatb.2013.05.077

[8] J. Li, E. Liu, Y. Ma, X. Hu, J. Wan, L. Sun, J. Fan, Appl. Surf. Sci. 364 (2016) 694-702; https://doi.org/10.1016/j.apsusc.2015.12.236

[9] M.S. Akple, J. Low, S. Wageh, A. A. Al-Ghamdi, J. Yu, J. Zhang, Appl. Surf. Sci. 358 (2015) 196-203; https://doi.org/10.1016/j.apsusc.2015.08.250

[10] X. Yang, H. Huang, M. Kubota, Z. He, N. Kobayashi, X. Zhou, J. Luo, Mater. Res. Bull. 76 (2016) 79-84; https://doi.org/10.1016/j.materresbull.2015.12.009

[11] C. T. Zhu, F. Chen, W. Yan, Y. C. Wei, J. Xu, Y. P. Chen, Chalcogenide Lett. 20 (2023) 685-695; https://doi.org/10.15251/CL.2023.209.685

[12] J. Xu, Q. Shi, H. Tang, C.S. Li, Dig. J. Nanomater. Biostructures. 10 (2015) 505-511.

[13] M.C. Liu, P. Ye , M. Wang , L.L. Wang , C. Wu, J. Xu, J Environ Chem Eng. 10(2022), 108436; https://doi.org/10.1016/j.jece.2022.108436

[14] J. Xu, P. Ye, Y.W. Cheng, Lei Ji, Y.C. Wei, Y.P. Chen, ENERGY TECHNOL-GER. 11(2023), 2201452; https://doi.org/10.1002/ente.202201452

[15] Y.Y. Xu, W. Yan, X. Sun, G.G. Tang, Y.P. Chen, J. Xu, Ceram. Int. 48 (2022) 7687-7694; https://doi.org/10.1016/j.ceramint.2021.11.316

[16] W. Yan, Y.Y. Xu, S.W. Hao, Z.D. He, L.L. Wang, Q.Y. Wei, J. Xu, H. Tang, Inorg. Chem. 61 (2021) 4725-4734; https://doi.org/10.1021/acs.inorgchem.2c00045

[17] J. Xu, Y.Y. Xu, G.G. Tang, H. Tang, H.B. Jiang, Appl. Surf. Sci. 492 (2019) 37-44; https://doi.org/10.1016/j.apsusc.2019.05.139

[18] J. Xu, H. Tang, Q. Shi, C.S. Li, Chalcogenide Lett. 12 (2015) 1-10.

[19] X.Y. Gao, P. Lu, Z.M. Xu, G.G. Tang, Chalcogenide Lett. 19 (2022) 513-527; https://doi.org/10.15251/CL.2022.198.513

[20] F.L. Sun, Y.L. Song, H. Tang, J. Xu, Chalcogenide Lett. 19 (2022) 371-379; https://doi.org/10.15251/CL.2022.195.371

[21] J.S. Hu, L.L. Ren, Y.G. Guo, H.P. Liang, A.M. Cao, L.J. Wan, C.L. Bai, Angew. Chem. Int. Ed. 117 (2005) 1295-1299; https://doi.org/10.1002/ange.200462057

[22] J.J. Kang, C.B. Wang, H.D. Wang, B.S. Xu, J.J. Liu, G.L. Li, Appl. Surf. Sci. 258 (2012) 1940-1943; https://doi.org/10.1016/j.apsusc.2011.06.149

[23] L. Chang, Z. Zhang, L. Ye, K. Friedrich, Tribol. Int. 40 (2007) 1170-1178; https://doi.org/10.1016/j.triboint.2006.12.002

[24] Ertan R, Yavuz N, Ind. Lubr. Tribol. 63 (2011) 245-253; https://doi.org/10.1108/00368791111140468

[25] W. Liu, S. Chen, Wear. 238 (2000) 120-124; https://doi.org/10.1016/S0043-1648(99)00344-0

[26] G. Liao, S. Chen, X. Quan, H. Yu, H. Zhao, J. Mater. Chem. A. 22 (2012) 2721-2726; https://doi.org/10.1039/C1JM13490F

[27] S. Liu, X. Zhang, H. Shao, J. Xu, F. Chen, Y. Feng, Mater. Lett. 73 (2012) 223-225; https://doi.org/10.1016/j.matlet.2012.01.024

[28] H. Liu, F. Zhang, W. Li, X. Zhang, C.S. Lee, W. Wang, Y. Tang, Electrochim. Acta. 167 (2015) 132-138; https://doi.org/10.1016/j.electacta.2015.03.151

[29] F. Maugé, J. Lamotte, N. S. Nesterenko, O. Manoilova, A. A. Tsyganenko, Catal. Today. 70 (2001) 271-284; https://doi.org/10.1016/S0920-5861(01)00423-0

[30] Y. Hanifehpour, B. Soltani, A. R. Amani-Ghadim, B. Hedayati, B. Khomami, S. W. Joo, J. Ind. Eng. Chem. 34 (2016) 41-50; https://doi.org/10.1016/j.jiec.2015.10.032

[31] W. Qin, D. Li, X. Zhang, D. Yan, B. Hu, L. Pan, Electrochim. Acta. 191 (2016) 435-443; https://doi.org/10.1016/j.electacta.2016.01.116

[32] W. Fu, H. He, Z. Zhang, C. Wu, X. Wang, H. Wang, Z. Liu, Nano Energy. 27 (2016) 44-50; https://doi.org/10.1016/j.nanoen.2016.06.037

[33] H. Zhao, Y. Dong, P. Jiang, H. Miao, G. Wang, J. Zhang, J. Mater. Chem. A. 3 (2015) 7375-7381; https://doi.org/10.1039/C5TA00402K